INSTITUTE OF PHYSICS PUBLISHING JOURNAL OF PHYSICS B: ATOMIC, MOLECULAR AND OPTICAL PHYSICS

J. Phys. B: At. Mol. Opt. Phys. **34** (2001) 2935–2949 PII: S0953-4075(01)19635-5

Differential cross sections for near-threshold electron impact dissociation of molecular hydrogen

Cynthia S Trevisan and Jonathan Tennyson

Department of Physics and Astronomy, University College London, Gower St, London WC1E 6BT, UK

Received 30 November 2000, in final form 27 April 2001
Published 18 July 2001
Online at stacks.iop.org/JPhysB/34/2935

Abstract

At low energies, the major pathway for the electron impact dissociation of H_2 is through excitation to b $^3\Sigma_u^+$. *Ab initio* calculations using the adiabatic nuclei, energy balance model of Stibbe and Tennyson (1998 *New J. Phys.* **1** 2.1) of total cross sections, angular differential cross sections, energy differential cross sections and double differential cross sections for the electronic ground state initial vibrational $v = 0$ level, dissociating into continuum states are presented. The formal expressions needed for such calculations, which involve three fragments in the exit channel, are derived.

1. Introduction

Electron impact dissociation of molecular hydrogen is considered to be a major route to molecular break-up in cool hydrogen plasmas (Kushner 1998, Fantz *et al* 1999). Such plasmas are found in a number of astrophysical environments and in the divertor region of tokamak fusion plasmas. In all cases, it is the rate of electron impact dissociation in the near-threshold region which is the important physical quantity.

Experimentally it is difficult to measure cross sections (or rates) for electron impact dissociation of a neutral species into neutral fragments. Only limited experimental data are available for this process (Corrigan 1965, Khakoo and Segura 1994, Nishimura and Danjo 1986, Hall and Andrić 1984), all of them for H_2 in its $v = 0$ vibrational ground state. However, calculations by Stibbe and Tennyson (1998a, 1999) have shown that the rate of near-threshold electron impact dissociation is strongly dependent on the initial vibrational state of H_2.

Although velocity distributions of final states within the context of dissociative autoionization of H_2 and D_2 have been studied classically (Hazi 1974, Hazi and Wiemers 1977), until now there has been no theoretical work on differential cross sections for electron impact dissociation. Differential cross sections are of interest for two reasons. Most of the near-threshold experimental measurements of the dissociation cross sections actually measured angular differential cross sections over a limited range of angles. A more rigorous test of any theory is therefore given by a direct comparison at the angular differential cross section level,

rather than by comparing with integral cross sections which are only determined experimentally with large uncertainties.

A break-up process, such as electron impact dissociation, also has an energy differential cross section. Although the energy with which the H atoms are created is of considerable interest for models of cool hydrogen plasmas (Kushner 1998, Tawara *et al* 1987, Matveyev and Silakov 1995, Silakov *et al* 1996), there appears to have been no previous work, either experimental or theoretical, on the energy differential cross section for the electron impact dissociation of H_2. Indeed, there appears not even to be a proper theoretical formulation for this process, although related processes in nuclear physics have been studied (Ohlsen 1965, Tostevin *et al* 1998). The outlines of a general theory which accounts for all the possible excitations of the molecule by electron impact but excludes break-up (ionization or dissociation) have also been presented (Shugard and Hazi 1975)

In this paper we formulate the differential cross section for electron impact dissociation in terms of T-matrices. We use the adiabatic nuclei approximation and the energy balance model of Stibbe and Tennyson (1998a) to obtain the appropriate energy-dependent T-matrices. This model assumes that the dissociation of H_2 for energies below around 12 eV proceeds exclusively via electronic excitation to the first excited state of H_2:

$$e^- + H_2(^1\Sigma_g^+) \rightarrow H_2^*(b\,^3\Sigma_u^+) + e^- \rightarrow H(1s) + H(1s) + e^-. \tag{1}$$

Our formulation of the problem leads to a slightly different expression for the total electron impact dissociation cross section to that of Stibbe and Tennyson (1998a). In practice this results in cross sections about 10% higher than those obtained previously using the same, bondlength-dependent T-matrix data (Stibbe and Tennyson 1998b). Our angular differential cross sections can be compared directly with measurements and, for the first time, we present energy differential cross sections.

2. Theory

Consider the electron impact dissociation of a molecule XY,

$$XY + e^- \rightarrow X + Y + e^-. \tag{2}$$

To describe the three particles in the final state of this break-up process, we adopted Jacobi coordinates. Parameters that refer to the outgoing electron are labelled with subscript e and, for the purpose of generality, those denoting the outgoing atoms with subscripts X and Y. Let the three particles have masses m_e, m_X, m_Y and position vectors $\boldsymbol{r}_e$, $\boldsymbol{r}_X$ and $\boldsymbol{r}_Y$, respectively (which are referred to an arbitrary fixed or uniformly moving origin). We define the following coordinates:

$$\boldsymbol{s} = m_e\boldsymbol{r}_e + m_X\boldsymbol{r}_X + m_Y\boldsymbol{r}_Y \tag{3}$$

$$\boldsymbol{s}_{e\text{–}XY} = \boldsymbol{r}_e - \frac{m_X\boldsymbol{r}_X + m_Y\boldsymbol{r}_Y}{m_X + m_Y} \tag{4}$$

$$\boldsymbol{s}_{X\text{–}Y} = \boldsymbol{r}_X - \boldsymbol{r}_Y \tag{5}$$

and reduced masses:

$$\mu_{e\text{–}XY} = \frac{m_e(m_X + m_Y)}{M} \tag{6}$$

$$\mu_{X\text{–}Y} = \frac{m_X m_Y}{m_X + m_Y} \tag{7}$$

$$M = m_e + m_X + m_Y. \tag{8}$$

The total kinetic energy $E_{\rm tot}$ in this arbitrary coordinate system is

$$E_{\rm tot} = \frac{p^2_{\rm e\text{–}XY}}{2\mu_{\rm e\text{–}XY}} + \frac{p^2_{\rm X\text{–}Y}}{2\mu_{\rm X\text{–}Y}} + \frac{P^2}{2M} = E_{\rm e\text{–}XY} + E_{\rm X\text{–}Y} \tag{9}$$

since $\boldsymbol{P} = 0$ in the centre-of-mass system.

According to the previous definitions (Ohlsen 1965, Tostevin *et al* 1998), the differential cross section for the break-up in Jacobi coordinates may be written as

$$\frac{{\rm d}^2\sigma}{{\rm d}\Omega_{\rm e\text{–}XY}\,{\rm d}E_{\rm e\text{–}XY}} = \frac{2\pi}{\hbar^2}\frac{\mu_{\rm e\text{–}XY}}{k_{\rm e}}|T_{\nu\to{\rm c}}(E_{\rm tot}, E_{\rm e\text{–}XY})|^2\rho(E_{\rm e\text{–}XY}) \tag{10}$$

with $\hbar\boldsymbol{k}_{\rm e}$ the relative momentum of the electron and XY target. ρ is referred to as the 'phase space factor' or as the 'density of final states'. $T_{\nu\to{\rm c}}$ represents the T-matrices associated with the transition from bound state ν to the continuous state c of XY.

Starting from a constant cross section in the phase space of the six independent variables involved, the density of final states will be proportional to the total number of 'states' available to the three final particles and is given by Fuchs (1982) as

$${\rm d}\sigma = h^{-6}\,{\rm d}^3p_{\rm e\text{–}XY}\,{\rm d}^3p_{\rm X\text{–}Y}\,\delta(E_{\rm tot} - A) \tag{11}$$

where $E_{\rm tot}$ is fixed at a value A. The only constraint assumed so far is the total available kinetic energy. This constraint introduces a relation between $E_{\rm e\text{–}XY}$ and $E_{\rm X\text{–}Y}$ and allows $E_{\rm X\text{–}Y}$ to be eliminated by integration over $E_{\rm X\text{–}Y}$, leaving only five independent variables ($E_{\rm e\text{–}XY}$ and four angles). Using coordinate transformations (table 1 of Fuchs (1982)), we can write equation (11) as

$$\begin{aligned}{\rm d}\sigma &= h^{-6}p^2_{\rm e\text{–}XY}\,{\rm d}p_{\rm e\text{–}XY}\,{\rm d}\Omega_{\rm e\text{–}XY}p^2_{\rm X\text{–}Y}\,{\rm d}p_{\rm X\text{–}Y}\,{\rm d}\Omega_{\rm X\text{–}Y}\delta(E_{\rm tot} - A)\\ &= h^{-6}p_{\rm e\text{–}XY}\mu_{\ \rm e\text{–}XY}\,{\rm d}E_{\rm e\text{–}XY}\,{\rm d}\Omega_{\rm e\text{–}XY}p_{\rm X\text{–}Y}\mu_{\rm X\text{–}Y}\,{\rm d}E_{\rm X\text{–}Y}\,{\rm d}\Omega_{\rm X\text{–}Y}\,\delta(E_{\rm tot} - A)\\ &= h^{-6}p_{\rm e\text{–}XY}\mu_{\rm e\text{–}XY}p_{\rm X\text{–}Y}\mu_{\rm X\text{–}Y}\,{\rm d}\Omega_{\rm e\text{–}XY}\,{\rm d}\Omega_{\rm X\text{–}Y}\,{\rm d}E_{\rm X\text{–}Y}\,{\rm d}E_{\rm tot}\,\delta(E_{\rm tot} - A).\end{aligned} \tag{12}$$

Following Ohlsen (1965) and Fuchs (1982),

$$\begin{aligned}\rho(E_{\rm e\text{–}XY}) &= \frac{{\rm d}\sigma}{{\rm d}\Omega_{\rm e\text{–}XY}\,{\rm d}E_{\rm e\text{–}XY}\,{\rm d}\Omega_{\rm X\text{–}Y}}\\ &= \int\frac{{\rm d}\sigma}{{\rm d}\Omega_{\rm e\text{–}XY}\,{\rm d}E_{\rm e\text{–}XY}\,{\rm d}\Omega_{\rm X\text{–}Y}\,{\rm d}E_{\rm X\text{–}Y}}\,{\rm d}E_{\rm X\text{–}Y}\,{\rm d}\Omega_{\rm X\text{–}Y}\\ &= 4\pi h^{-6}\int p_{\rm e\text{–}XY}\mu_{\rm e\text{–}XY}p_{\rm X\text{–}Y}\mu_{\rm X\text{–}Y}\,\delta(E_{\rm tot} - A)\,{\rm d}E_{\rm X\text{–}Y}\\ &= 4\pi h^{-6}\int p_{\rm e\text{–}XY}\mu_{\rm e\text{–}XY}p_{\rm X\text{–}Y}\mu_{\rm X\text{–}Y}\,\delta(E_{\rm tot} - A)\frac{{\rm d}E_{\rm tot}}{\partial E_{\rm tot}/\partial E_{\rm X\text{–}Y}}\\ &= 4\pi h^{-6}\mu_{\rm e\text{–}XY}\mu_{\rm X\text{–}Y}\left[\frac{p_{\rm e\text{–}XY}p_{\rm X\text{–}Y}}{\partial E_{\rm tot}/\partial E_{\rm X\text{–}Y}}\right]_{E_{\rm tot}=A}.\end{aligned} \tag{13}$$

However,

$$\frac{\partial E_{\rm tot}}{\partial E_{\rm X\text{–}Y}} = \frac{\partial E_{\rm tot}}{\partial p_{\rm X\text{–}Y}}\frac{\partial p_{\rm X\text{–}Y}}{\partial E_{\rm X\text{–}Y}}. \tag{14}$$

Thus, using equation (9),

$$\frac{\partial E_{\rm tot}}{\partial E_{\rm X\text{–}Y}} = p_{\rm X\text{–}Y}(2\mu_{\rm X\text{–}Y}E_{\rm X\text{–}Y})^{-1/2} = p_{\rm X\text{–}Y}p^{-1}_{\rm X\text{–}Y} = 1.$$

We finally obtain

$$\rho(E_{\text{e–XY}}) = 4\pi h^{-6}\mu_{\text{e–XY}}\mu_{\text{X–Y}}p_{\text{e–XY}}p_{\text{X–Y}}. \tag{15}$$

In terms of energy,

$$\rho(E_{\text{e–XY}}) = 2^{-3}(\pi)^{-5}(\hbar)^{-6}(\mu_{\text{e–XY}}\mu_{\text{X–Y}})^{3/2}(E_{\text{e–XY}}E_{\text{X–Y}})^{1/2} \tag{16}$$

or

$$\rho(E_{\text{e–XY}}) = 2^{-3}(\pi)^{-5}(\hbar)^{-6}\left(\frac{m_{\text{e}}m_{\text{X}}m_{\text{Y}}}{M}\right)^{3/2}[E_{\text{e–XY}}(E_{\text{tot}} - E_{\text{e–XY}})]^{1/2}. \tag{17}$$

This expression for ρ can now be used in the expression for the double differential cross sections, equation (10), to obtain a general, double differential, break-up cross section in terms of T-matrices:

$$\frac{\mathrm{d}^2\sigma}{\mathrm{d}\Omega_{\text{e–XY}}\,\mathrm{d}E_{\text{e–XY}}} = \frac{\mu_{\text{e–XY}}}{4\pi^4\hbar^8 k_{\text{e}}}\left(\frac{m_{\text{e}}m_{\text{X}}m_{\text{Y}}}{M}\right)^{3/2}[E_{\text{e–XY}}(E_{\text{tot}} - E_{\text{e–XY}})]^{1/2}|T_{v\to\text{c}}(E_{\text{tot}}, E_{\text{e–XY}})|^2. \tag{18}$$

Recasting this general break-up expression into the notation used by Stibbe and Tennyson (1998a) for the electron impact dissociation of H_2, $E_{\text{e–XY}} = E_{\text{out}}$ represents the energy of the scattered electron; $E_{\text{tot}} = E_{\text{in}} - D_v$, where E_{in} is the energy of the incoming electron and D_v is the vibrational state-dependent dissociation energy; $E_{\text{X–Y}} = E_{\text{ke}}$, where E_{ke} is the kinetic energy of the dissociating atoms. Finally, $m_{\text{X}} = m_{\text{Y}} = m_{\text{H}}$, where m_{e} and m_{H} are the masses of the electron and hydrogen nucleus, respectively.

$\hbar\boldsymbol{k}_{\text{e}}$, the relative momentum of the electron and XY target, can be approximated by $\boldsymbol{p}_{\text{e}}$, assuming the standard Born–Oppenheimer approximation based on $(m_{\text{X}} + m_{\text{Y}}) \gg m_{\text{e}}$. With this, the double differential cross section can be expressed as

$$\frac{\mathrm{d}^2\sigma}{\mathrm{d}\Omega\,\mathrm{d}E_{\text{out}}} = \frac{m_{\text{e}}^2 m_{\text{H}}^{3/2}}{16\pi^4\hbar^7}\frac{E_{\text{out}}^{1/2}(E_{\text{in}} - D_v - E_{\text{out}})^{1/2}}{E_{\text{in}}^{1/2}}|T_{v\to\text{c}}(E_{\text{in}}, E_{\text{out}})|^2 \tag{19}$$

or, in terms of the scattering amplitude, $f_{v\to\text{c}}$,

$$\frac{\mathrm{d}^2\sigma}{\mathrm{d}\Omega\,\mathrm{d}E_{\text{out}}} = \frac{m_{\text{H}}^{3/2}}{4\pi^4\hbar^3}\frac{E_{\text{out}}^{1/2}(E_{\text{in}} - D_v - E_{\text{out}})^{1/2}}{E_{\text{in}}^{1/2}}|f_{v\to\text{c}}(E_{\text{in}}, E_{\text{out}})|^2 \tag{20}$$

where use has been made of the following relation between T-matrices and scattering amplitudes (Morrison and Sun 1995):

$$T_{ij} = \frac{\mathrm{i}\hbar^2}{2\pi m_{\text{e}}}f_{ij}. \tag{21}$$

Equation (21) depends upon the normalization used and upon the choice of relationships between the scattering matrices $\boldsymbol{S}$ and transition matrices $\boldsymbol{T}$. We use $\boldsymbol{T} = \boldsymbol{S} - 1$ and unit normalization. For a further discussion on this topic, see Morrison and Sun (1995).

Stibbe and Tennyson (1998a) proposed an energy balance model which generalized the adiabatic nuclei approximation to the break up problem of electron impact dissociation. Within their model, T-matrices for transitions to the continuum are obtained from fixed-nuclei inelastic (off-shell) T-matrices by

$$T_{v\to\text{c}}(E_{\text{in}}, E_{\text{out}}) = \langle \Xi_c(E_{\text{ke}}, R)|T_{ij}(\epsilon(R) + E_{\text{out}}, E_{\text{out}}, R)|\Xi_v(R)\rangle \tag{22}$$

where R represents the internuclear distance or bondlength, and $\epsilon(R)$ is the fixed-nuclei or vertical target electronic excitation energy. Ξ_v represent bound nuclear wavefunctions and Ξ_c represent continuum nuclear wavefunctions. Stibbe and Tennyson used energy-normalized continuum function (in atomic units),

$$\Xi_c(R \to \infty) \sim \left(\frac{2\mu}{\pi k}\right)^{1/2} \sin(kR + \delta). \tag{23}$$

However, in order to be consistent with the expressions derived above for the double differential cross sections and angular differential cross sections formulae discussed below, Ξ_c needs to be momentum normalized. Thus, when using Ξ_c from Stibbe and Tennyson, we need to include a correction factor, ξ^2, such that

$$\xi^2 = 2\hbar \left(\frac{E_{\mathrm{ke}}}{m_{\mathrm{H}}}\right)^{1/2}. \tag{24}$$

We used the standard energy-normalized asymptotic form of the wavefunction for an electron incident upon a neutral molecule, which can be found, for instance, in Burke (1982), equation (5) or Malegat (1990), equation (1) and is consistent with the treatment given by Friedrich (1990).

The relation between the scattering amplitudes, f_{ij}, and the transition matrices, T_{ij}, has been derived by Burke (1982) and is used by Malegat (1990). Malegat developed a computational code that calculates, among other things, angular differential cross sections, $\mathrm{d}\sigma/\mathrm{d}\Omega$, for elastic and inelastic scattering. According to Malegat's expressions (6) and (7), we can write

$$|f_{ij}|^2 = \frac{k_i}{k_j} \sum_t A^t_{\bar{i}\bar{j}} P_t(\cos\theta) \tag{25}$$

where i, j label the initial and final electronic states of the molecule, respectively, and A^t_{ij} are coefficients given by Malegat's equation (8):

$$\begin{aligned} A^t_{\bar{i}\bar{j}} = \frac{(-1)^{\Lambda_i+\Lambda_j}}{8(2t+1)(2S_i+1)k_i^2} \sum_{\substack{\Lambda\nu\bar{l}_i\bar{l}_j \\ \Lambda'\nu'\bar{l}'_i\bar{l}'_j}} \mathrm{i}^{\bar{l}_i-\bar{l}_j-\bar{l}'_i+\bar{l}'_j} \left[(2\bar{l}_i+1)(2\bar{l}'_i+1)(2\bar{l}_j+1)(2\bar{l}'_j+1)\right]^{1/2} \\ \times (\bar{l}_i 0 \bar{l}'_i 0 \mid k0)(\bar{l}_j 0 \bar{l}'_j 0 \mid k0)(\bar{l}_i \Lambda_i - \Lambda \bar{l}'_i \Lambda' - \Lambda \mid k\Lambda' - \Lambda) \\ \times (\bar{l}_j \Lambda_j - \Lambda \bar{l}'_j \Lambda' - \Lambda \mid k\Lambda' - \Lambda) \sum_S (2S+1) T^{\Lambda S\nu}_{\bar{i}\bar{l}_i\bar{j}\bar{l}_j} T^{\Lambda' S\nu' *}_{\bar{i}\bar{l}'_i\bar{j}\bar{l}'_j} \end{aligned} \tag{26}$$

where the indices i, j denote all quantum numbers needed to specify the electronic state i, j of the molecule, respectively. $\bar{i}$, $\bar{j}$ denote (Λ_i, S_i, ν_i) and (Λ_j, S_j, ν_j), and $\bar{l}_i$, $\bar{l}_j$ run over values satisfying $(-1)^{\bar{l}_i}\nu_i = \nu$; $(-1)^{\bar{l}_j}\nu_j = \nu$; S represents the total spin and ν labels the gerade or ungerade symmetry in homonuclear molecules. Primed coordinates refer to the molecular frame (MF), with the z'-axis along the interatomic axis and unprimed coordinates to the laboratory frame (LF), with the z-axis along the incident beam. The 3-j coefficients are those of Messiah (1960). Thus,

$$|f_{v\to \mathrm{c}}(E_{\mathrm{in}}, E_{\mathrm{out}})|^2 = \frac{E_{\mathrm{in}}^{1/2}}{E_{\mathrm{out}}^{1/2}} \sum_t A^t_{\bar{i}\bar{j}}(E_{\mathrm{in}}, E_{\mathrm{out}}) P_t(\cos\theta). \tag{27}$$

Substituting (24) and (27) into (20), we obtain

$$\frac{\mathrm{d}^2\sigma}{\mathrm{d}\Omega\,\mathrm{d}E_{\mathrm{out}}} = \frac{m_{\mathrm{H}}}{2\pi^4\hbar^2}(E_{\mathrm{in}} - D_v - E_{\mathrm{out}}) \sum_t A^t_{\bar{i}\bar{j}}(E_{\mathrm{in}}, E_{\mathrm{out}}) P_t(\cos\theta). \tag{28}$$

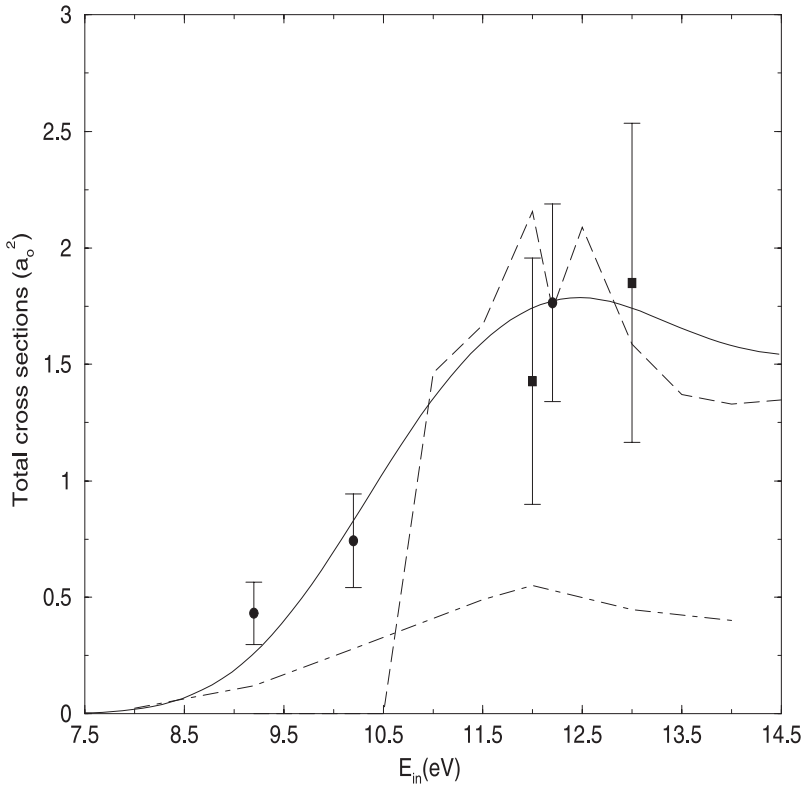

Figure 1. Electron impact dissociation cross sections for $H_2(v = 0)$ as a function of the incoming electron energy, $E_{\rm in}$. Full circles with error bars are measurements from Khakoo and Segura (1994). Squares with error bars are measurements from Nishimura and Danjo (1986). The full curve represents our calculations and the broken curve represents the fixed-nuclei model. The chain curve represents total cross sections using the classical δ-function approximation for the final continuum vibrational function.

Integrating (28) over solid angle $\mathrm{d}\Omega$ will give

$$\frac{\mathrm{d}\sigma}{\mathrm{d}E_{\rm out}} = \frac{m_{\rm H}}{2\pi^4\hbar^2}(E_{\rm in} - D_v - E_{\rm out})4\pi A^0_{\bar{i}\bar{j}}(E_{\rm in}, E_{\rm out})$$
$$= \frac{m_{\rm H}}{8\pi^3 m_{\rm e}}\frac{(E_{\rm in} - D_v - E_{\rm out})}{E_{\rm in}}\sum_{\Lambda v\bar{l}_i\bar{l}_j S}(2S+1)\left|T^{\Lambda v S}_{\bar{i}\bar{l}_i\bar{j}\bar{l}_j}(E_{\rm in}, E_{\rm out})\right|^2 \qquad (29)$$

or, in terms of the kinetic energy of the dissociating H atoms,

$$\frac{\mathrm{d}\sigma}{\mathrm{d}E_{\rm ke}} = \frac{m_{\rm H}}{8\pi^3 m_{\rm e}}\frac{E_{\rm ke}}{E_{\rm in}}\sum_{\Lambda v l_i l_j S}(2S+1)\left|T^{\Lambda S v}_{\bar{i}\bar{l}_i\bar{j}\bar{l}_j}(E_{\rm in}, E_{\rm ke})\right|^2. \qquad (30)$$

For the angular differential cross sections, we can use Malegat's expression (7):

$$\frac{\mathrm{d}\sigma}{\mathrm{d}\Omega} = \sum_t A^t_{\bar{i}\bar{j}}(E_{\rm in})P_t(\cos\theta) \qquad (31)$$

where

$$A^t_{\bar{i}\bar{j}}(E_{\rm in}) = \frac{m_{\rm H}}{2\pi^4\hbar^2}\int_0^{E_{\rm in}-D_v}(E_{\rm in} - D_v - E_{\rm out})A^t_{\bar{i}\bar{j}}(E_{\rm in}, E_{\rm out})\,\mathrm{d}E_{\rm out}. \qquad (32)$$

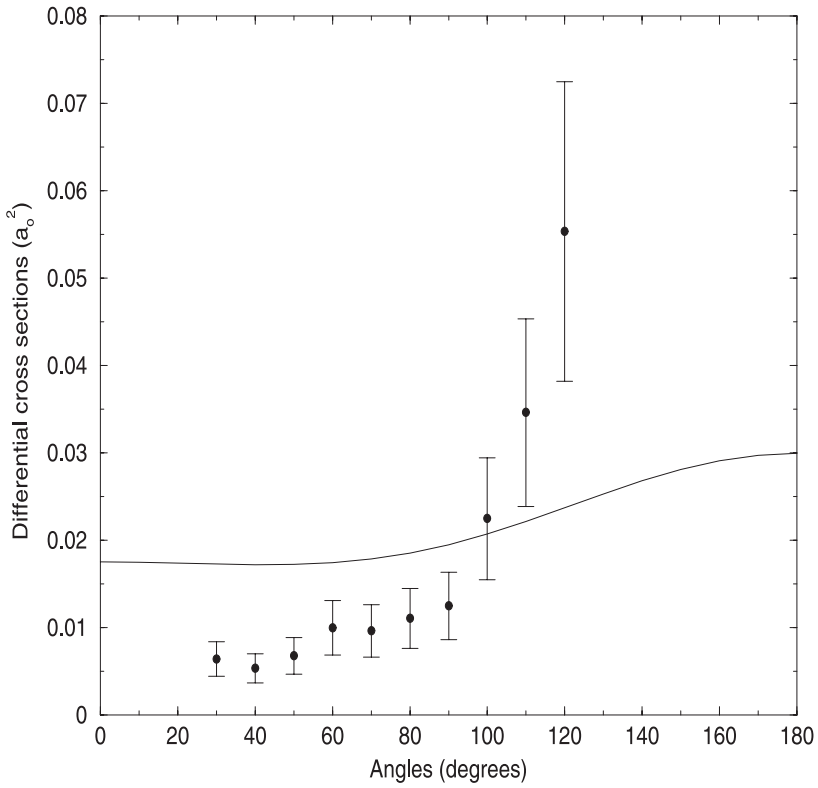

Figure 2. Angular differential cross sections for impact dissociation of $H_2(v = 0)$ by an incoming electron energy of 9.2 eV. The full curve represents our model, which includes nuclear motion. Full circles with error bars represent experimental values from Khakoo and Segura (1994).

Finally, for the total cross sections we used

$$\sigma(E_{\rm in}) = \int_0^{E_{\rm in}-D_v} \frac{{\rm d}\sigma}{{\rm d}E_{\rm out}}\,{\rm d}E_{\rm out}. \tag{33}$$

At the same time,

$$\sigma(E_{\rm in}) = A^0_{\bar{i}\bar{j}}(E_{\rm in}). \tag{34}$$

Total cross sections have been calculated by both methods as a numerical check of our procedure.

3. Method

In the particular case of dissociation of molecular hydrogen from the $X\,^1\Sigma_g^+$ ground state, only $S = \frac{1}{2}$ will survive, and this will reduce equation (29) to

$$\frac{{\rm d}\sigma}{{\rm d}E_{\rm out}} = \frac{m_{\rm H}}{4\pi^3 m_{\rm e}} \frac{(E_{\rm in} - D_v - E_{\rm out})}{E_{\rm in}} \sum_{\Lambda v l_i l_j} \left| T^{\Lambda v}_{\bar{i}\bar{l}_i \bar{j}\bar{l}_j}(E_{\rm in}, E_{\rm out}) \right|^2. \tag{35}$$

The T-matrices used here were originally calculated in an investigation of H_2^- resonances as a function of the internuclear distance R (Stibbe and Tennyson 1997a, b, 1998b).

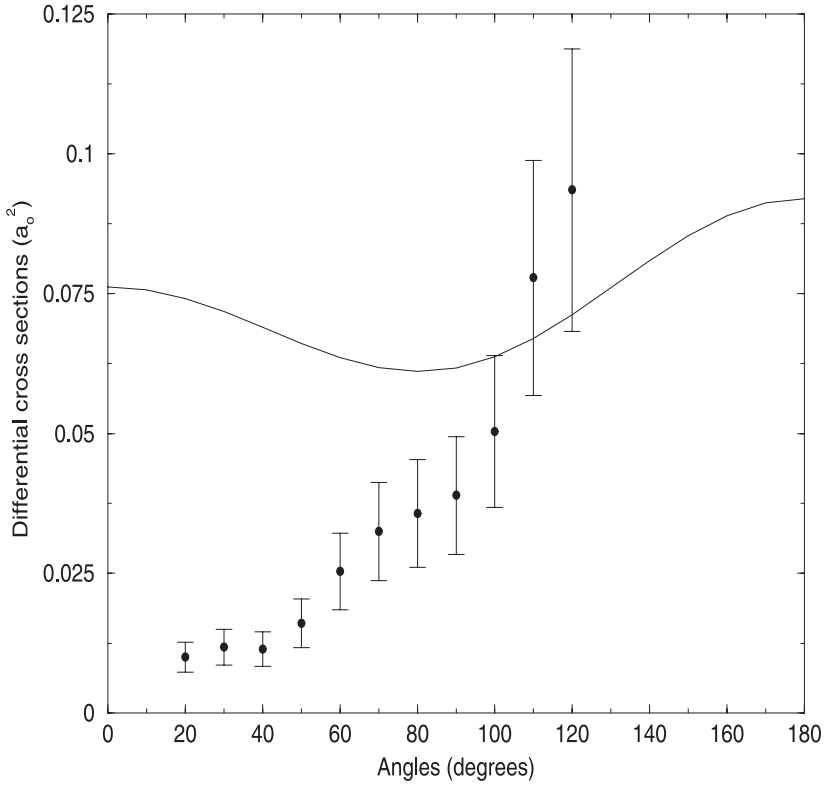

Figure 3. Angular differential cross sections for impact dissociation of $H_2(v = 0)$ by an incoming electron energy of 10.2 eV. The full curve represents our model, which includes nuclear motion. Full circles with error bars represent experimental values from Khakoo and Segura (1994).

Calculations were performed for R ranging from 0.8 a_0 to 4.0 a_0 in steps of 0.1 a_0 using the UK Molecular R-matrix suite of programs (Gillan *et al* 1995). Target wavefunctions were represented using a full configuration interaction (CI) within a basis set of $4\sigma_g$, $3\sigma_u$, $3\pi_u$ and $3\pi_g$ Slater-type orbitals (STOs) which have been energy optimized (Stibbe and Tennyson 1998b) for the lowest seven target states (X $^1\Sigma_g^+$, b $^3\Sigma_u^+$, a $^3\Sigma_g^+$, B $^1\Sigma_u^+$, C $^1\Pi_u$, c $^3\Pi_u$, E, F $^1\Sigma_g^+$), those retained in our close-coupling expansion. Numerical functions were used to represent the continuum electron in a truncated ($l \leqslant 6$, $m \leqslant 3$) partial-wave expansion. Such calculations yielded full T-matrices linking all the (open) target states included in the calculation; in this particular case only the off-diagonal portion of the matrix which links the X $^1\Sigma_g^+$ and b $^3\Sigma_u^+$ states is of interest. Full details can be found in Stibbe and Tennyson (1998b).

As the excitation is from a singlet to a triplet state, it is exchange dominated and rapidly convergent with total symmetry. Only the lowest four total symmetries, $^2\Sigma_g^+$, $^2\Sigma_u^+$, $^2\Pi_u$ and $^2\Pi_g$, were included. Stibbe and Tennyson found higher symmetries gave a negligible contribution to the internal cross section, in accordance with previous calculations (Baluja *et al* 1985, Branchett *et al* 1991). Nevertheless, we performed a symmetry convergence check over a range of energies for the incoming electron in order to analyse how much the inclusion of four further symmetries would affect angular differential cross sections. After performing calculations of angular differential cross sections with a total of four and then eight total symmetries and having found that differences between these calculations were within an

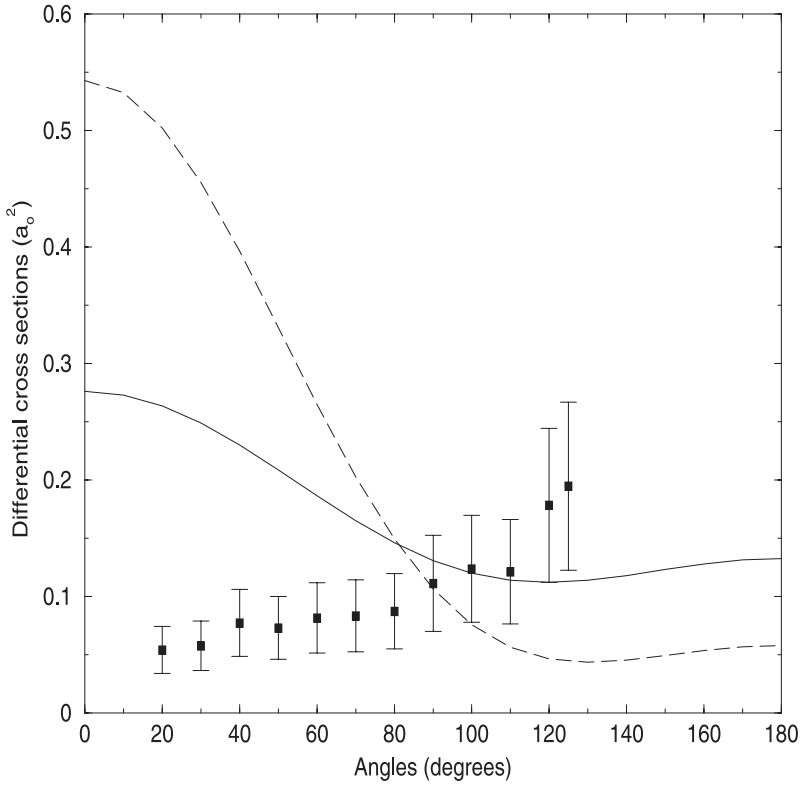

Figure 4. Angular differential cross sections for impact dissociation of $H_2(v = 0)$ by an incoming electron energy of 12 eV. The full curve represents our model, which includes nuclear motion. The broken curve represents the fixed-nuclei model. Squares with error bars represent experimental values from Nishimura and Danjo (1986).

acceptable range (between 0 and 7.7%) the decision to include only the lowest four symmetries when analysing angular information was justified.

In Stibbe and Tennyson's model, the low-lying $^2\Sigma_u^+$ shape resonance does not contribute non-adiabatically, but that omission is not expected to make any measurable difference (Atems and Wadehra 1993). Due to its short lifetime ($\Gamma \sim 1$ eV), the adiabatic treatment of the B $^2\Sigma_g^+$ H_2^- resonance associated with the b $^3\Sigma_u^+$ dissociative state should be sufficient. In practice, the largest contribution comes from the non-resonant $^2\Sigma_u^+$ symmetry in line with previous calculations (Rescigno and Schneider 1988, Atems and Wadehra 1993). Nevertheless, poor differential cross sections reopen the issue of the contribution of resonances to this process in the near-threshold region, as was recently highlighted by Xu *et al* (2000). Tests using our results showed that doubling the $^2\Sigma_u^+$ contribution to the differential cross sections gave differential cross sections significantly closer in form to experiment, but somewhat too high.

Nuclear continuum wavefunctions, $\Xi_c(E_{ke}, R)$, were calculated by solving the Schrödinger equation directly for the dissociating potential, and energy normalized according to the asymptotic condition stated in equation (23). The exact potential of Kolos and Wolniewicz (1965) was used in place of that implicit in the T-matrix calculations, which is (~ 0.1 eV) less accurate. The initial vibrational wavefunctions and energies were found with the program LEVEL (Le Roy 1996) also using the exact potential. For each value of E_{out},

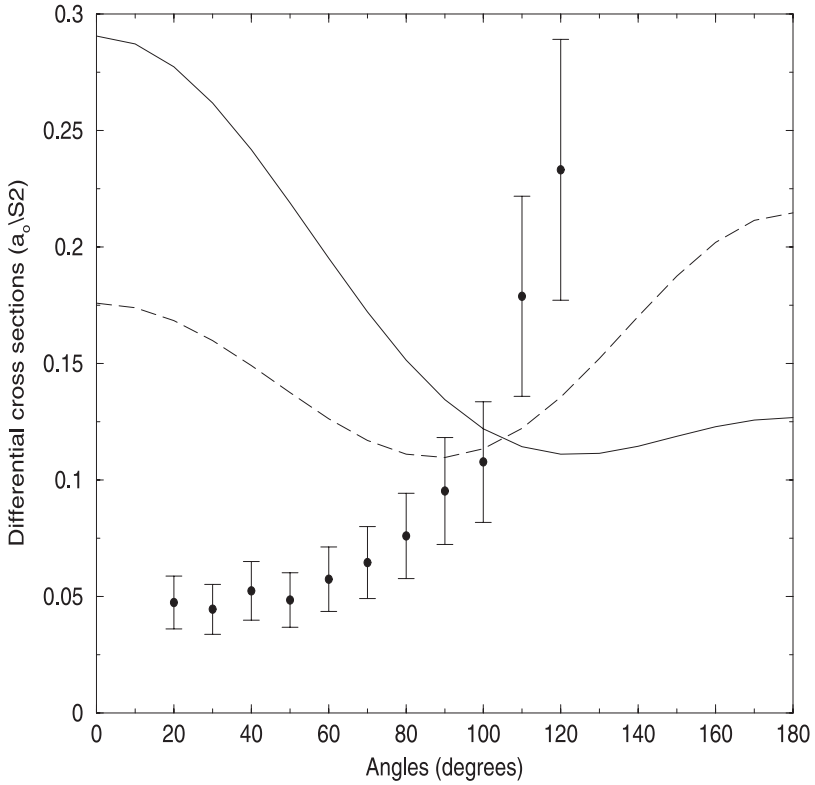

Figure 5. Angular differential cross sections for impact dissociation of $H_2(v = 0)$ by an incoming electron energy of 12.2 eV. The full curve represents our model, which includes nuclear motion. The broken curve represents the fixed-nuclei model. Full circles with error bars represent experimental values from Khakoo and Segura (1994).

the appropriate fixed-nuclei T-matrices were interpolated over 1000 points between $R = 0.8$ and 4.0 a_0 prior to numerical integration to account for the rapid oscillations of the continuum functions.

4. Results and discussion

Figure 1 shows the dissociation cross sections for $H_2(v = 0)$ as a function of incoming electron energy. Although cross sections are shown up to 14.5 eV, our calculations, represented by the full curve, are expected to be accurate only up to around 12 eV. Above that energy, the molecule can be excited to higher states from which it can dissociate directly or cascade down to the repulsive state. Another possibility above 12 eV is the excitation of an H_2 resonance state which can then decay into the b $^3\Sigma_u^+$ state. The adiabatic model we use is not valid for these long-lived resonances and cannot model the additional dissociation pathways above 12 eV.

In the region where this model is valid, there are few available experimental results. Those that are available have very wide error bars. The agreement with the measurements of Khakoo and Segura (1994) is good considering the large experimental uncertainties, with errors ranging from 22% to 31%. The agreement with the cross sections of Nishimura and Danjo (1986),

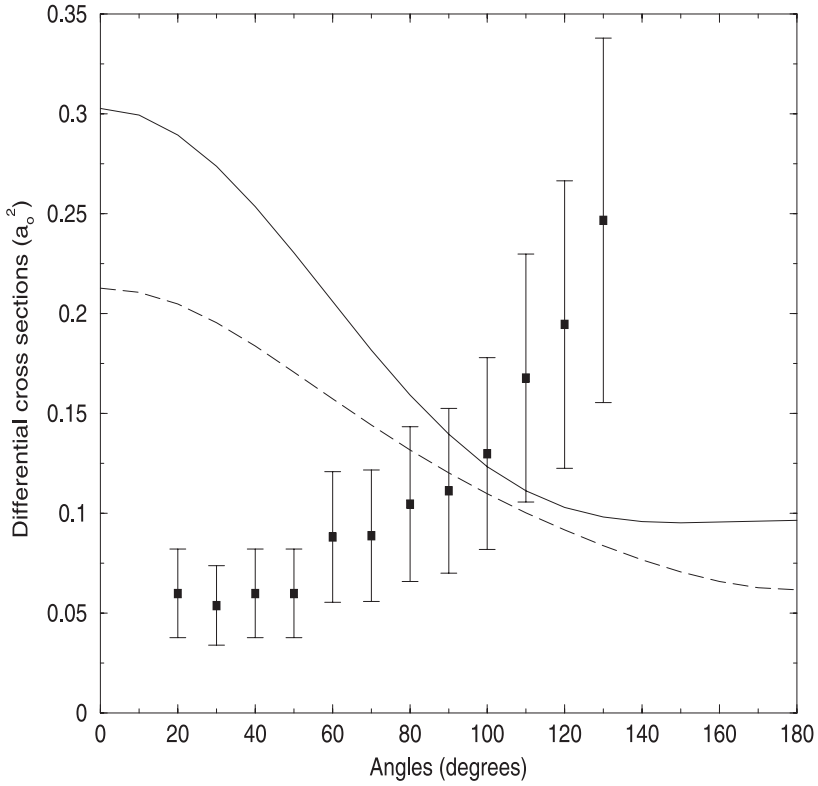

Figure 6. Angular differential cross sections for impact dissociation of $H_2(v = 0)$ by an incoming electron energy of 13 eV. The full curve represents our model, which includes nuclear motion. The broken curve represents the fixed-nuclei model. Squares with error bars represent experimental values of Nishimura and Danjo (1986).

with estimated errors of about $\pm 37\%$, is also good, although their results are in energy ranges just above the region of validity of this model (12 eV). As expected at higher energies, our calculations underestimate the experimental values, due to the additional dissociation pathways that are not being taken into account.

Also shown in the figure are calculations performed using the fixed-nuclei model at the equilibrium bond length for molecular hydrogen ($R = 1.4\ a_0$), represented by a broken curve. Note that the dissociation cross section drops to zero below its vertical target electronic excitation energy of 10.5 eV. This model cannot predict dissociation cross sections below that threshold.

Most previous calculations (Fliflet and McKoy 1980, Baluja *et al* 1985, Schneider and Collins 1985, Lima *et al* 1985, Parker *et al* 1991, Branchett *et al* 1990) have been performed at the H_2 equilibrium bond length and do not take into account the nuclear motion. Rescigno and Schneider (1988) performed a series of two-state, fixed-nuclei calculations using the Kohn variational method to find R-dependent T-matrices which they averaged using an initial vibrational and a δ-function approximation to a final continuum function. However, they made no allowance for the variation in the vertical excitation energy with R, and took no account of energy partitioning between the outgoing atoms and the exciting electron. This prevents their method from being used near the effective Franck–Condon threshold.

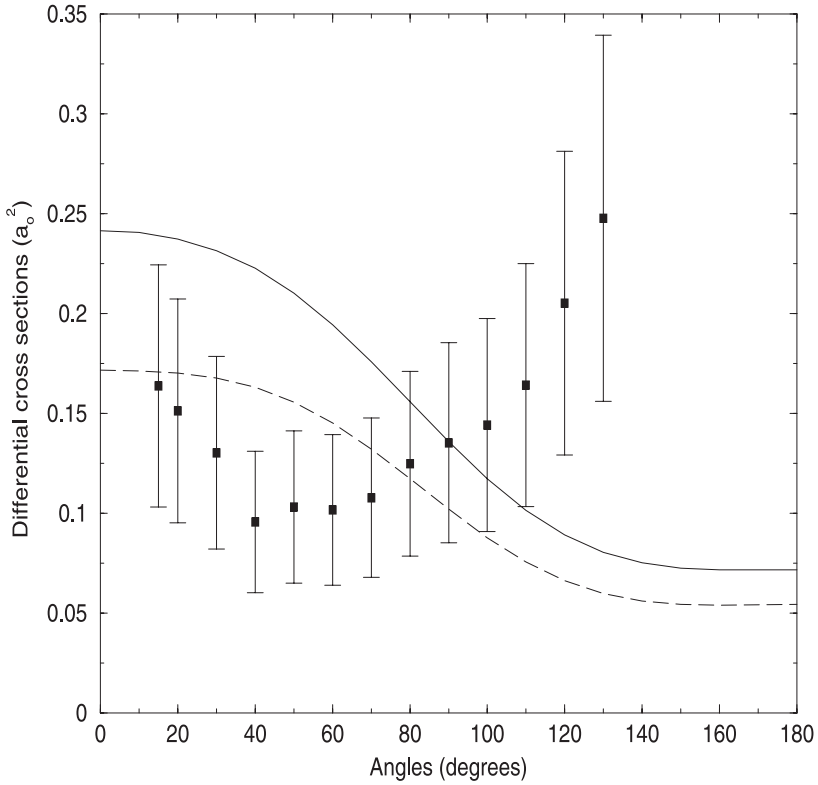

Figure 7. Angular differential cross sections for impact dissociation of $H_2(v = 0)$ by an incoming electron energy of 15 eV. The full curve represents our model, which includes nuclear motion. The broken curve represents the fixed-nuclei model. Squares with error bars represent experimental values from Nishimura and Danjo (1986).

Celiberto *et al* used the semiclassical Gryzinski approximation to look at the dissociation of H_2 (Celiberto *et al* 1989) and D_2 (Celiberto *et al* 1990), again using a δ-function approximation for the continuum, which they suggest should be useful for a qualitative comparison. Gorse *et al* (1992) also used the Gryzinski approximation and by adjusting parameters within that approximation gained good agreement with experiment at higher energies. The method they used for the nuclear dynamics is not well documented, making it difficult to judge the accuracy of their near-threshold results. For comparison purposes, we have also included total cross sections using the classical δ-function approximation for the final continuum vibrational function in figure 1, represented by the chain curve. Such an approximation appears to significantly underestimate the total cross sections, suggesting that the approximate treatment of the continuum nuclear wavefunction is inappropriate for a light system near threshold.

The vertical target electronic excitation energy (or fixed-nuclei energy) at the outer classical turning point for the vibrational ground state of H_2 using the exact potential curves is 8.7 eV. Within our model, this means that any dissociation found at electron energies below this arises via tunnelling, for which this model explicitly allows. The effective Franck–Condon threshold region has not been well characterized experimentally, although there are indications in the results of both Nishimura and Danjo (1986) and Khakoo and Segura (1994) that it lies below 8.7 eV.

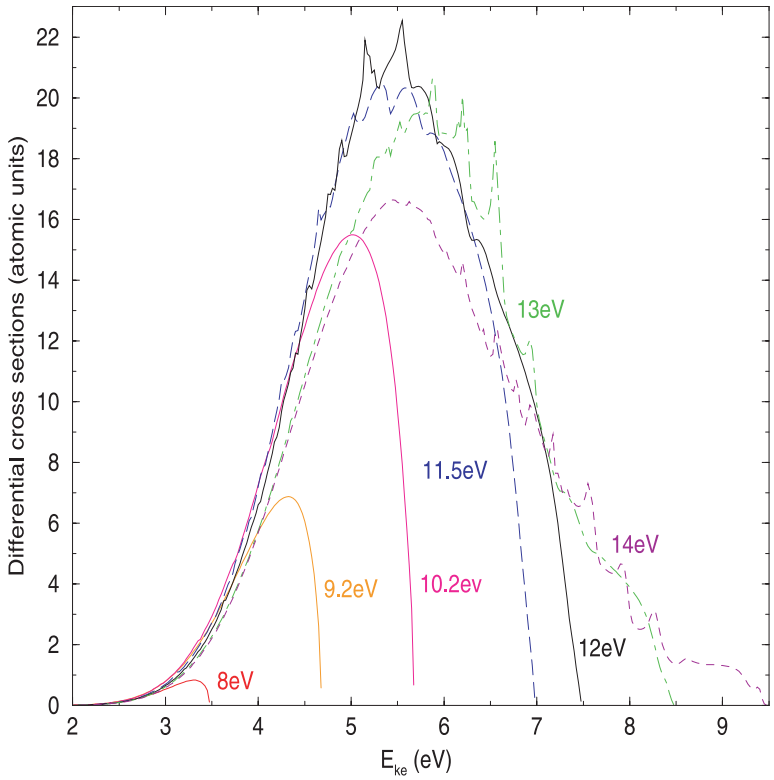

Figure 8. Energy differential cross sections electron impact dissociation of $H_2(v = 0)$ as a function of the energy of the dissociating atoms for different values of incoming electron energies.
(This figure is in colour only in the electronic version, see `www.iop.org`)

Figures 2–7 illustrate angular differential cross sections for different values of incoming electron energy. The full curve represents our calculations; the broken curve represents the fixed-nuclei model. Full circles with error bars represent the available experimental values. At energies below 10.5 eV the fixed-nuclei model cannot predict dissociation cross sections. As expected, above 12 eV our results do not model the experimental results properly.

Figure 8 shows energy differential cross sections as a function of the energy of the dissociating atoms for different values of incoming electron energies. At low energies (below 12 eV), most of the available energy above dissociation is carried away by the dissociating hydrogen atoms. This suggests that electron impact dissociation is unlikely to be the source of anomalously cold H atoms which have been found in a number of hydrogen plasmas (Hey *et al* 1996, 1999, 2000, Mertens and Silz 1997).

5. Conclusions

Up until now, models for the electron impact dissociation of molecular hydrogen found it difficult to predict experimental cross sections near threshold energies. Our calculations provide a better agreement with experiment than previous models at electron energies below 12 eV.

Integral cross sections were found to give good agreement with experimental results. We were also able to model dissociation at electron energies below the classical turning point value by taking into account the effects of tunnelling. The poorer angular differential cross sections reopen the issue of the contribution of resonances to this process in the near-threshold region.

We presented, for the first time, energy differential cross section electron impact dissociation of $H_2(v = 0)$ as a function of the energy of the dissociating atoms for different values of incoming electron energies. Our results suggest that this process is unlikely to explain the presence of the cold H atoms which have been found in a number of hydrogen plasmas.

Although calculations have been carried out only for the initial vibrational ground state ($v = 0$), we expect to find a strong dependence of the thermal rate of dissociation on initial vibrational states, in accordance with Stibbe and Tennyson's (1998a) results. Currently, we are performing calculations for further initial vibrational levels and extending our work to also describe the dissociation of deuterium and tritium.

Acknowledgments

We wish to thank Thornton Greenland, David Moores, Lesley Morgan, Darian Stibbe and Jeff Tostevin for useful discussions and guidance.

References

Atems D E and Wadehra J M 1993 *J. Phys. B: At. Mol. Opt. Phys.* **26** L759
Baluja K L, Noble C J and Tennyson J 1985 *J. Phys. B: At. Mol. Phys.* **18** L851
Branchett S E, Tennyson J and Morgan L A 1990 *J. Phys. B: At. Mol. Opt. Phys.* **23** 4625–39
——1991 *J. Phys. B: At. Mol. Opt. Phys.* **24** 3479–90
Burke P G 1982 *Atomic and Molecular Collisions Theory* ed F A Gianturco (New York: Plenum)
Celiberto R, Cacciatore M, Capitelli M and Gorse C 1989 *Chem. Phys.* **133** 355
Celiberto R, Cives P, Cacciatore M, Capitelli M and Lamanna U T 1990 *Chem. Phys. Lett.* **169** 69
Corrigan S J B 1965 *J. Chem. Phys.* **43** 4381–6
Fantz U, Behringer K, Gafert J and Coster D 1999 *J. Nucl. Mater.* **269** 490–4
Fliflet V and McKoy V 1980 *Phys. Rev.* A **21** 1863
Friedrich A 1990 *Theoretical Atomic Physics* (Berlin: Springer)
Fuchs H 1982 *Nucl. Instrum. Methods* **200** 361–8
Gillan C J, Tennyson J and Burke P G 1995 *Computational Methods for Electron–Molecule Collisions* ed W M Huo and F Gianturco (New York: Plenum)
Gorse C, Celiberto R, Cacciatore M, Laganà A and Capitelli M 1992 *Chem. Phys.* **161** 211
Hall R I and Andrić L 1984 *J. Phys. B: At. Mol. Phys.* **17** 3815–25
Hazi A U 1974 *J. Chem. Phys.* **60** 4358–61
Hazi A U and Wiemers K 1977 *J. Chem. Phys.* **66** 5296–305
Hey J D, Chu C C and Hintz E 1999 *J. Phys. B: At. Mol. Opt. Phys.* **32** 3555–73
——2000 *Contrib. Plasma Phys.* **40** 9–22
Hey J D, Korten M, Lie Y T, Pospieszczyk A, Rusbueldt D, Schweer B, Unterberg B, Wienbeck J and Hintz E 1996 *Contrib. Plasma Phys.* **36** 583–604
Khakoo M A and Segura J 1994 *J. Phys. B: At. Mol. Opt. Phys.* **27** 2355–68
Kolos W and Wolniewicz L 1965 *J. Chem. Phys.* **43** 2429
Kushner M J 1998 *Abstracts of DAMOP* (*Santa Fe, 1998*)
Le Roy R J 1996 *University of Waterloo Chemical Physics Research Report* CP-555R, p 1
Lima M A P, Gibson T L, Huo W M and McKoy V 1985 *J. Phys. B: At. Mol. Phys.* **18** L865
Malegat L 1990 *Comput. Phys. Commun.* **60** 391–404
Matveyev A A and Silakov V P 1995 *Plasma Sources Sci. Technol.* **4** 606
Mertens P and Silz M 1997 *J. Nucl. Mater.* **241–3** 842–7
Messiah A 1960 *Mecanique Quantique* (Paris: Dunod)
Morrison M A and Sun W 1995 *Computational Methods for Electron–Molecule Collisions* ed W M Huo and F A Gianturco (New York: Plenum)

Nishimura H and Danjo A 1986 *J. Phys. Soc. Japan* **55, 9** 3031–6
Ohlsen G G 1965 *Nucl. Instrum. Methods* **37** 240–8
Parker S D, McCurdy C W, Rescigno T N and Lengsfield B H 1991 *Phys. Rev.* A **43** 3514
Rescigno T N and Schneider B I 1988 *J. Phys. B: At. Mol. Opt. Phys.* **21** L691
Schneider B I and Collins L A 1985 *J. Phys. B: At. Mol. Phys.* **18** L857
Shugard M and Hazi A U 1975 *Phys. Rev.* A **12** 1895–902
Silakov V P, Matveyev A A, Chebotarev A V and Otorbaev D K 1996 *J. Phys. D: Appl. Phys.* **29** 2111
Stibbe D T and Tennyson J 1997a *Phys. Rev. Lett.* **79** 4116
——1997b *J. Phys. B: At. Mol. Opt. Phys.* **30** L301
——1998a *New J. Phys.* **1** 2.1–2.9
——1998b *J. Phys. B: At. Mol. Opt. Phys.* **31** 815
——1999 *Astrophys. J.* **513** L147–50
Tawara H, Itakawa Y, Nishimura H and Yoshino M 1987 *Report* IPPJ-AM-55, Institute of Plasma Physics, Nagoya University
Tostevin J A, Rugmai S and Johnson R C 1998 *Phys. Rev.* C **57** 3225–36
Xu Y, Kazansky A K and Fabrikant I I 2000 *Phys. Rev.* A **63** 014703